Quasi-Affine Transformation in 3-D: Theory and Algorithms

David Coeurjolly, Valentin Blot, Marie-Andrée Jacob-da Col

Quasi-Affine Transformation in 3-D: Theory and Algorithms

David Coeurjolly[1], Valentin Blot[2] and Marie-Andrée Jacob-Da Col[3]

[1] Université de Lyon, CNRS, LIRIS, UMR5205, F-69622, France
david.coeurjolly@liris.cnrs.fr
[2] Ecole Normale Supérieure de Lyon valentin.blot@ens-lyon.fr
[3] LSIIT-UMR 7005, Pôle API Bd Sébastien Brant, Illkirch, F-67412, France
dacolm@iutlpa.u-strasbg.fr

Abstract. In many applications and in many fields, algorithms can considerably be speed up if the underlying arithmetical computations are considered carefully. In this article, we present a theoretical analysis of affine transformations in dimension 3. More precisely, we investigate the arithmetical paving induced by the transformation to design fast algorithms.

Key words: quasi-affine transform, periodic tiling, arithmetic, image transformation.

1 Introduction

In many computer vision and image processing applications, we are facing new constraints due to the image sizes both in dimension with 3-D and 3-D+t medical acquisition devices, and in resolution with VHR (Very High Resolution) satellite images. This article deals with high performance image transformations using quasi-affine transforms (QATs for short), which can be viewed as a discrete version of general affine transformations. QAT can approximate rotations and scalings, and in some specific cases, QAT may also be one-to-one and onto mappings from $\mathbb{Z}^n$ to $\mathbb{Z}^n$, leading to exact computations. In dimension 2, the QAT appeared in several articles [1,2,3,4,5]. In higher dimension, theoretical results have been demonstrated [6,7,8]. More precisely, authors have demonstrated the arithmetical and periodic structures embedded in $n-$dimensional QAT, leading to generic transformation algorithms. To implement these generic algorithms, several elements have to be fixed when considering a specific dimension. In this paper, we detail the computation of the minimal periods in dimension 3 leading to efficient transformation algorithms. Due to the space limitation, the proofs are available in the technical report [7]). In Section 2, we first present some definitions and results on $n-$D QAT. Section 3 focuses on the parameter computation in 3-D. Finally, Section 4 evaluate all the algorithms compared to a classical backward-mapping technique [9].

2 Preliminaries

In this section, we present definitions and results obtained for QAT in higher dimension. These results have been independently proved by [6] and [7,8]. In the following, we consider notations introduced in [7,8]. Let n denote the dimension of the considered space, V_i the i^{th} coordinate of vector V, and $M_{i,j}$ the $(i,j)^{th}$ coefficient of matrix M. We use the notation $\gcd(a,b,\ldots)$ for the greatest common divisor of an arbitrary number of arguments, and $\mathrm{lcm}(a,b,\ldots)$ for their least common multiple. Let $\left[\frac{a}{b}\right]$ denote the quotient of the euclidean division of a by b, that is the integer $q \in \mathbb{Z}$ such that $a = bq + r$ satisfying $0 \leq r < |b|$ regardless of the sign of b[4]. We also consider the straightforward generalization of these operators to $n-$dimensional vectors (*e.g.* $\left[\frac{V}{b}\right]$ is a vector where each component is the quotient of the division by b).

Definition 1. *A quasi-affine transformation is a triple* $(\omega, M, \boldsymbol{V}) \in \mathbb{Z} \times M_n(\mathbb{Z}) \times \mathbb{Z}^n$ *(we assume that* $\det(M) \neq 0$*). The associated application is :*

$$\begin{aligned} \mathbb{Z}^n &\longrightarrow \mathbb{Z}^n \\ X &\longmapsto \left[\frac{MX+V}{\omega}\right] \end{aligned}$$

Definition 2. *The inverse of a QAT* (ω, M, V) *is the QAT:*

$$(\det(M), \omega \operatorname{com}(M)^t, -\operatorname{com}(M)^t V)\,, \tag{1}$$

where M^t *denotes the transposed matrix and* $\operatorname{com}(M)$ *the co-factor matrix of* M *(Remind that* $M \operatorname{com}(M)^t = \operatorname{com}(M)^t M = \det(M) I_n$*.).*

The associated affine application of the inverse of a QAT is therefore the inverse of the affine application associated to the QAT. However, due to the nested floor function, the composition $f \cdot f^{-1}$ is not the identity function in the general case. Let us recall the well-known Bezout Identity:

$$\forall (a,b) \in \mathbb{Z}^2, \exists (u,v) \in \mathbb{Z}^2 / au + bv = \gcd(a,b)\,.$$

In Section 3, we have to consider a generalized form of the Bezout identity in dimension 3:

Proposition 1 ([7]). $\forall (a,b,c) \in \mathbb{Z}^3, \exists (u,v,w) \in \mathbb{Z}^3 / au + bv + cw = \gcd(a,b,c)\,.$

We present now several results and definitions that have been presented for $n-$dimensional QAT. All these results are given in [7,8] but we present here the main theorems, which will be used in the rest of the paper. First, the key feature of $n-$D QAT is that it contains a periodic paving structure.

Definition 3 (Tile). *Let* f *be a QAT. For* $Y \in \mathbb{Z}^n$*, we denote:*

$$P_Y = \{X \in \mathbb{Z}^n / f(X) = Y\}\,, \tag{2}$$

P_Y *is called order 1 tile of index* Y *of* f*.*

[4] $\left\{\frac{a}{b}\right\}$ denotes the corresponding remainder $\left\{\frac{a}{b}\right\} = a - b\left[\frac{a}{b}\right]$.

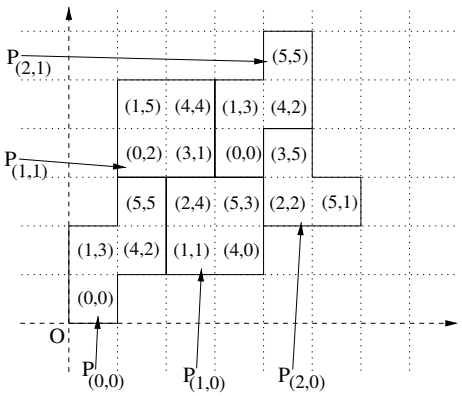

Fig. 1. Example of tiles and remainders

Definition 4. *P_Y is said arithmetically equivalent to P_Z (denoted $P_Y \equiv P_Z$) if:*

$$\forall X \in P_Y, \exists X' \in P_Z / \left\{ \frac{MX+V}{\omega} \right\} = \left\{ \frac{MX'+V}{\omega} \right\} . \tag{3}$$

Definition 5. *P_Y and P_Z are said geometrically equivalent if:*

$$\exists \boldsymbol{v} \in \mathbb{Z}^n / P_Y = T_{\boldsymbol{v}} P_Z \, , \tag{4}$$

where $T_{\boldsymbol{v}}$ denotes the translation of vector $\boldsymbol{v}$.

The following theorem exhibits a relation between the notions of arithmetically and geometrically equivalent tiles.

Theorem 1 ([7,8]). *If $P_Y \equiv P_Z$, then P_Y and P_Z are geometrically equivalent. Since $P_Y \equiv P_Z$, there exists $X \in P_Y$ and $X' \in P_Z$ such that:*

$$\left\{ \frac{MX+V}{\omega} \right\} = \left\{ \frac{MX'+V}{\omega} \right\} .$$

Then $\boldsymbol{v} = X - X'$ is the translation vector:

$$P_Y = T_{\boldsymbol{v}} P_Z \, .$$

In Figure 1 we show some tiles of the QAT defined by $(6, \begin{pmatrix} 3 & 1 \\ -1 & 3 \end{pmatrix}, \begin{pmatrix} 0 \\ 0 \end{pmatrix})$ (a point of $\mathbb{Z}^2$ is represented by a unit square whose bottom-left corner corresponds to the represented point). For each point X in a tile we provide its corresponding remainder $\left\{ \frac{MX+V}{\omega} \right\}$. Tiles $P_{(2,1)}$ and $P_{(0,0)}$ are arithmetically equivalent, therefore they are also geometrically equivalent. It should also be noted that tiles $P_{(1,0)}$ and $P_{(1,1)}$ are geometrically equivalent but they are not arithmetically equivalent .

Definition 6 (Periodicity notations, [7,8]). *For all $0 \leq i < n$, We define the set $\mathcal{A}_i$ as follows:*

$$\mathcal{A}_i = \{\alpha \in \mathbb{N}^* / \exists (\beta_j)_{0 \leq j < i} \in \mathbb{Z}^i, \forall (y_0, \ldots, y_{n-1}) \in \mathbb{Z}^n, \\ P_{y_0,\ldots,y_i+\alpha,\ldots,y_{n-1}} \equiv P_{y_0+\beta_0,\ldots,y_{i-1}+\beta_{i-1},y_i,\ldots,y_{n-1}}\}$$

Furthermore, let us consider $\alpha_i = \min(\mathcal{A}_i)$. We define $\{\beta_j^i\}_{0 \leq j < i} \in \mathbb{Z}^i$ and $U_i \in \mathbb{Z}^n$ such that

$$\forall (y_0, \ldots, y_{n-1}) \in \mathbb{Z}^n, P_{y_0,\ldots,y_i+\alpha_i,\ldots,y_{n-1}} = T_{\boldsymbol{U_i}} P_{y_0+\beta_0^i,\ldots,y_{i-1}+\beta_{i-1}^i,y_i,\ldots,y_{n-1}}\,.$$

The key theorem for the QAT periodic structure can now be presented:

Theorem 2 (Periodicity, [7,8]). *The set of QAT tiles is $n-$periodic, in other words*

$$\forall 0 \leq i < n, \mathcal{A}_i \neq \emptyset$$

Let us suppose that quantities α_i, β_j^i and U_i are given. The following theorem allows us to obtain P_Y as the translation of a canonical tile P_{Y^0}.

Theorem 3 ([7,8]). *$\forall (y_0, \ldots, y_{n-1}) \in \mathbb{Z}^n$, we have $P_{y_0,\ldots,y_{n-1}} = T_W P_{y_0^0,\ldots,y_{n-1}^0}$ with*

$$W = \sum_{i=0}^{n-1} w_i U_i \quad \textit{and} \quad \forall n > i \geq 0, \begin{cases} w_i = \left\lceil \frac{y_i + \sum_{j=i+1}^{n-1} w_j \beta_i^j}{\alpha_i} \right\rceil \\ y_i^0 = \left\{ \frac{y_i + \sum_{j=i+1}^{n-1} w_j \beta_i^j}{\alpha_i} \right\} \end{cases} .$$

In [7,8], we have proved that canonical tiles P_{Y^0} are associated to grid points of a special tile called *super-tile*.

Definition 7 (Super-tile, [7,8]). *A super-tile of a QAT is the set $\mathcal{P}$ such that*

$$\mathcal{P} = \bigcup_{0 \leq Y^0 < (\alpha_0,\ldots,\alpha_{n-1})} P_{Y^0}$$

Theorem 4 ([7,8]). *$\mathcal{P}$ is the tile $P_{(0,\ldots,0)}$ of the QAT defined by:*

$$\left(\omega \operatorname{lcm}_{0 \leq i < n}(\alpha_i), \begin{pmatrix} \theta_0 & \cdots & 0 \\ \vdots & \ddots & \vdots \\ 0 & \cdots & \theta_{n-1} \end{pmatrix} M, \begin{pmatrix} \theta_0 & \cdots & 0 \\ \vdots & \ddots & \vdots \\ 0 & \cdots & \theta_{n-1} \end{pmatrix} V \right) ,$$

with $\forall 0 \leq i < n-1$, $\theta_i = \frac{\operatorname{lcm}_{0 \leq j < n-1}(\alpha_j)}{\alpha_i}$.

Figure 2 illustrates tiles of the QAT $(84, \begin{pmatrix} 12 & -11 \\ 18 & 36 \end{pmatrix}, \begin{pmatrix} 0 \\ 0 \end{pmatrix})$ in $\mathbb{Z}^2$ with 15 arithmetically distinct tiles (the tiles with same color are arithmetically equivalent). In this example, for all $i, j \in \mathbb{N}$, $P_{(i+5,j)} \equiv P_{(i,j)}$ and $P_{(i+2,j-3)} \equiv P_{(i,j)}$.

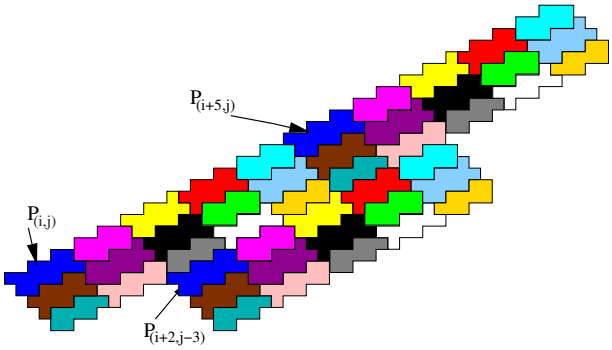

Fig. 2. Periodicity of thes tiles of a 2D QAT .

The set $\left\{P_{(i,j)} | i = 0, 1, 2, 3, 4, j = 0, 1, 2\right\}$ contains exactly once all distinct tiles so it is a super-tile of the QAT.

In [7,8], we have demonstrated that if we consider the Hermite Normal Form of the QAT matrix M, then efficient tile construction can be designed. In the following, let $MH = T$ denote the Hermite Normal Form (with $\det(H) = \pm 1$ and T upper triangular). Note that this form always exists for nonsingular integer square matrix.

Theorem 5 (Tile Construction, [7,8]). *$\forall Y \in \mathbb{Z}^n$, let $MH = T$ be the Hermite Normal Form of the QAT matrix M,*

$$P_Y = \{HX \ / \ \forall n > i \geq 0, A_i(X_{i+1}, \ldots, X_{n-1}) \leq X_i < B_i(X_{i+1}, \ldots, X_{n-1})\}$$

$$\begin{aligned} \textit{With } A_i(X_{i+1}, \ldots, X_{n-1}) &= -\left\lceil \frac{-\omega Y_i + \sum_{j=i+1}^{n-1} T_{i,j} X_j + V_i}{T_{i,i}} \right\rceil , \\ B_i(X_{i+1}, \ldots, X_{n-1}) &= -\left\lceil \frac{-\omega (Y_i + 1) + \sum_{j=i+1}^{n-1} T_{i,j} X_j + V_i}{T_{i,i}} \right\rceil . \end{aligned}$$

In Algorithm 1, we give the generic algorithm applying a contracting QAT f to an image $\mathcal{A}$ (see Fig. 3). The principle is that we give to each pixel Y of image $\mathcal{B}$ the average color of the tile P_Y in image $\mathcal{A}$. If f is a dilating QAT, we obtain a similar algorithm in which we replace f with f^{-1}, and then we give the color of each pixel Y of image $\mathcal{A}$ to each pixel of P_Y in image $\mathcal{B}$ (see Fig. 3 for an illustration in 2-D). In both algorithms, some elements cannot be computed in arbitrary dimension n. Indeed, even if there exist algorithms to compute the Hermite Normal Form of an arbitrary square integer matrix [10], there is no generic algorithm to obtain the minimal periodicities $\{\alpha_i\}$ (see discussion in Sect. 5). In the next section, we focus on the minimal periodicity computation in dimension 3.

Algorithm 1: Generic QAT algorithm for a contracting QAT

Input: a contracting QAT $f := (\omega, M, \boldsymbol{V})$, an image $\mathcal{A} : \mathbb{Z}^n \to \mathbb{Z}$
Output: a transformed image $\mathcal{B} : \mathbb{Z}^n \to \mathbb{Z}$
Compute the Hermite Normal Form of the matrix M;
Determine the minimal periodicities $\{\alpha_i\}$ and vectors $\{\boldsymbol{U}_i\}$;
Use Theorems 4 and 5 to compute the canonical tiles in the super-tile $\mathcal{P}$;
foreach $Y \in \mathcal{B}$ **do**
  Find Y^0 and W such that $P_Y = T_W P_{Y^0}$;
  foreach $Z \in P_{Y^0}$ **do**
    $c \leftarrow \mathcal{A}(T_W Z)$; `// we read the color in the initial image`
    $sum \leftarrow sum + c$;
  $\mathcal{B}(Y) \leftarrow sum/|P_{Y^0}|$; `// we set the color`

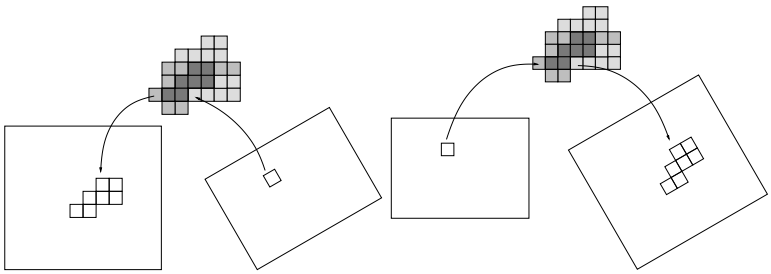

(a) (b)

Fig. 3. Illustration in dimension 2 of the QAT algorithm when f is contracting (a) and dilating (b). In both cases, we use the canonical tiles contained in the super-tile to speed-up the transformation.

3 QAT in Dimension 3

In dimension 3, we consider the following framework: we first define the Hermite Normal Form, the minimal periods and then we detail the transformation algorithm.

3.1 Hermite Normal Form and Tile Construction

Let us consider a QAT (ω, M, V) with $M = \begin{pmatrix} a_0 & b_0 & c_0 \\ d_0 & e_0 & f_0 \\ g_0 & h_0 & i_0 \end{pmatrix}$ and $V = \begin{pmatrix} j_0 \\ k_0 \\ l_0 \end{pmatrix}$.

In [7], we present explicit formulas to compute the Hermite Normal Form in 3-D. In the following, we define $H = H_1 H_2 H_3 H_4$ and $MH = T = \begin{pmatrix} a & b & c \\ 0 & d & e \\ 0 & 0 & f \end{pmatrix}$. Thanks to Hermite decomposition, we have $a > 0$, $d > 0$ and $f > 0$. To construct the tile of index (i, j, k) and thanks to Theorem 5, we have:

$$A_2 = -\left[\frac{-\omega k + l_0}{f}\right], B_2 = -\left[\frac{-\omega(k+1) + l_0}{f}\right]$$

$$A_1(z) = -\left\lceil \frac{-\omega j + k_0 + ez}{d} \right\rceil, B_1(z) = -\left\lceil \frac{-\omega(j+1) + k_0 + ez}{d} \right\rceil$$
$$A_0(y,z) = -\left\lceil \frac{-\omega i + j_0 + by + cz}{a} \right\rceil, B_0(y,z) = -\left\lceil \frac{-\omega(i+1) + j_0 + by + cz}{a} \right\rceil$$

Algorithm 2: Tile construction in 3-D

$A_2 \leftarrow -\left\lceil \frac{-\omega k + l_0}{f} \right\rceil$;
$B_2 \leftarrow -\left\lceil \frac{-\omega(k+1) + l_0}{f} \right\rceil$;
for $z \leftarrow A_2$ **to** B_2 - *1* **do**
  $A_1 \leftarrow -\left\lceil \frac{-\omega j + k_0 + ez}{d} \right\rceil$;
  $B_1 \leftarrow -\left\lceil \frac{-\omega(j+1) + k_0 + ez}{d} \right\rceil$;
  for $y \leftarrow A_1$ **to** B_1 - *1* **do**
    $A_0 \leftarrow -\left\lceil \frac{-\omega i + j_0 + by + cz}{a} \right\rceil$;
    $B_0 \leftarrow -\left\lceil \frac{-\omega(i+1) + j_0 + by + cz}{a} \right\rceil$;
    for $x \leftarrow A_0$ **to** B_0 - *1* **do**
      $H \begin{pmatrix} x \\ y \\ z \end{pmatrix} \in P_{i,j,k}$;

3.2 Minimal Periodicity and Super-tile Construction

In dimension 3, we need to compute the periodicity along each dimension. Let us first denote $a'_h = \frac{a}{\gcd(a,\omega)}, \omega'_h = \frac{\omega}{\gcd(a,\omega)}, Y = \begin{pmatrix} \omega'_h \\ 0 \\ 0 \end{pmatrix}$

Theorem 6 (Horizontal Periodicity). *Let $\alpha_h = a'_h$ and $U = HY$. Then $\alpha_h > 0$, $P_{i+\alpha_h,j,k} \equiv P_{i,j,k}$ and $\forall (i,j,k) \in \mathbb{Z}^3, P_{i+\alpha_h,j,k} = T_U P_{i,j,k}$.*

Proof. The proof is detailed in [7].

Theorem 7. *The period α_h is a minimal horizontal period,* i.e. $\alpha_h = \alpha_0$.

Proof. The proof is given in [7].

Concerning the vertical period, let:

$d'_v = \frac{d}{\gcd(d,\omega)}, \omega'_v = \frac{\omega}{\gcd(d,\omega)}, a'_v = \frac{a}{\gcd(a, b\omega'_v, \omega)}, \phi = \frac{b\omega'_v}{\gcd(a, b\omega'_v, \omega)}, \omega''_v = \frac{\omega}{\gcd(a, b\omega'_v, \omega)}$,
$\alpha'_v = \gcd(a'_v, \omega''_v)$, u_1 and v_1 are such that : $a'_v u_1 + \omega''_v v_1 = \gcd(a'_v, \omega''_v) (= \alpha'_v)$,
$\beta_0 = -\phi v_1, Y = \begin{pmatrix} -\phi u_1 \\ \omega'_v \alpha'_v \\ 0 \end{pmatrix}$

Theorem 8 (Vertical Periodicity). *Let* $\alpha_v = d'_v\alpha'_v, U = HY$. *Then* $\alpha_v > 0$, $P_{i,j+\alpha_v,k} \equiv P_{i+\beta_0,j,k}$ *and* $\forall (i,j,k) \in \mathbb{Z}^3, P_{i,j+\alpha_v,k} = T_U P_{i+\beta_0,j,k}$.

Proof. The proof is given in [7].

Theorem 9. *The period* α_v *is a minimal vertical period,* i.e. $\alpha_v = \alpha_1$.

Proof. The proof is detailled in [7].

For the last period, let us consider:

$$f'_d = \frac{f}{\gcd(\omega, f)}, \omega'_d = \frac{\omega}{\gcd(\omega, f)}, d'_d = \frac{d}{\gcd(d, e\omega'_d, \omega)}, \phi = \frac{e\omega'_d}{\gcd(d, e\omega'_d, \omega)}, \omega''_d = \frac{\omega}{\gcd(d, e\omega'_d, \omega)},$$

u_1 and v_1 are such that : $d'_d u_1 + \omega''_d v_1 = \gcd(d'_d, \omega''_d), \psi = c\omega'_d \gcd(d'_d, \omega''_d) - b\phi u_1,$

$$a'_d = \frac{a}{\gcd(a, \psi, \omega, \frac{\omega''_d b}{\gcd(d'_d, \omega''_d)})}, \psi' = \frac{\psi}{\gcd(a, \psi, \omega, \frac{\omega''_d b}{\gcd(d'_d, \omega''_d)})},$$

$$\omega'''_d = \frac{\omega}{\gcd(a, \psi, \omega, \frac{\omega''_d b}{\gcd(d'_d, \omega''_d)})}, \chi = \frac{\frac{\omega''_d b}{\gcd(d'_d, \omega''_d)}}{\gcd(a, \psi, \omega, \frac{\omega''_d b}{\gcd(d'_d, \omega''_d)})},$$

$\alpha''_d = \gcd(a'_d, \chi, \omega'''_d), \alpha'_d = \alpha''_d \gcd(d'_d, \omega''_d),$

u_2, v_2 and w_2 are such that : $a'_d u_2 + \chi v_2 + \omega'''_d w_2 = \gcd(a'_d, \chi, \omega'''_d) (= \alpha''_d),$

$$k = -\psi' v_2, \beta_0 = -\psi' w_2, \beta_1 = -\phi v_1 \alpha''_d - k\frac{d'_d}{\gcd(d'_d, \omega''_d)}, Y = \begin{pmatrix} -\psi' u_2 \\ -\phi u_1 \alpha''_d + k\frac{\omega''_d}{\gcd(d'_d, \omega''_d)} \\ \alpha'_d \omega'_d \end{pmatrix}$$

Theorem 10 (Depth Periodicity). *Let* $\alpha_d = \alpha'_d f'_d, U = HY$. *Then*

$$\alpha_d > 0 \quad P_{i,j,k+\alpha_d} \equiv P_{i+\beta_0,j+\beta_1,k} \quad \text{and } \forall (i,j,k) \in \mathbb{Z}^3, P_{i,j,k+\alpha_d} = T_U P_{i+\beta_0,j+\beta_1,k}$$

Proof. The proof is detailed in [7].

Theorem 11. *The period* α_d *is a minimal depth period,* i.e. $\alpha_d = \alpha_2$.

Proof. The proof is detailed in [7].

Based on these periods, we can construct the super-tile and all the initial period tiles. To design a transformation algorithm, for each point $X \in \mathcal{P}$, we need to determine the tile index Y to which X belongs to. Since $X \in P_Y \Leftrightarrow \left[\frac{MX+V}{\omega}\right] = Y$, Algorithm 3 details the initial period tile construction with scanning points in $\mathcal{P}$. The computational cost of Alg. 3 exactly corresponds to the number of tiles in the initial period.

Proposition 2. *The number of tiles of the initial period is* $\omega'_d \omega''_d \omega'''_d$.

In the Proposition statement, we do not give the closed formula. However, $\omega'_d \omega''_d \omega'''_d$ is equal to ω^3 divided by a product of three gcd().

Algorithm 3: Super-tile and initial period tiles construction in 3-D.

$A'_2 \leftarrow -\left\lceil \frac{l_0}{f} \right\rceil$;
for $z \leftarrow A'_2$ **to** $A'_2 + \frac{\omega\alpha_2}{f}$ *- 1* **do**
  $A'_1 \leftarrow -\left\lceil \frac{k_0+ez}{d} \right\rceil$;
  for $y \leftarrow A'_1$ **to** $A'_1 + \frac{\omega\alpha_1}{d}$ *- 1* **do**
    $A'_0 \leftarrow -\left\lceil \frac{j_0+by+cz}{a} \right\rceil$;
    for $x \leftarrow A'_0$ **to** $A'_0 + \frac{\omega\alpha_0}{a}$ *- 1* **do**
      $Y \leftarrow \left\lceil \frac{T\begin{pmatrix} x \\ y \\ z \end{pmatrix} + V}{\omega} \right\rceil$;
      $H \begin{pmatrix} x \\ y \\ z \end{pmatrix} \in P_Y$;

Proof. The proof is detailed in [7].

Using Theorems 4 and 5, we have

$$\theta_0 = \frac{\mathrm{lcm}(\alpha_0, \alpha_1, \alpha_2)}{\alpha_0}, \theta_1 = \frac{\mathrm{lcm}(\alpha_0, \alpha_1, \alpha_2)}{\alpha_1}, \theta_1 = \frac{\mathrm{lcm}(\alpha_0, \alpha_1, \alpha_2)}{\alpha_2},$$

and

$$\mathcal{P} = \left\{ H \begin{pmatrix} x \\ y \\ z \end{pmatrix} / A'_2 \leq z < B'_2, A'_1(z) \leq y < B'_1(z) \text{ and } A'_0(y,z) \leq x < B'_0(y,z) \right\},$$

with $A'_2 = -\left\lceil \frac{l_0}{f} \right\rceil, A'_1(z) = -\left\lceil \frac{k_0+ez}{d} \right\rceil, A'_0(y,z) = -\left\lceil \frac{j_0+by+cz}{a} \right\rceil$, $B'_2 = A'_2 + \frac{\omega\alpha_2}{f}$, $B'_1(z) = A'_1(z) + \frac{\omega\alpha_1}{d}$, and $B'_0(y,z) = A'_0(y,z) + \frac{\omega\alpha_0}{a}$ (see [7] for details).

Figure 4 shows the 16 distinct tiles of the QAT $(11, \begin{pmatrix} 6 & -2 & 3 \\ 2 & -2 & -3 \\ 4 & 4 & -4 \end{pmatrix}, \begin{pmatrix} 0 \\ 0 \\ 0 \end{pmatrix})$ in $\mathbb{Z}^3$ and its correponding super-tile.

3.3 QAT Algorithm in 3-D

To obtain the overall QAT algorithm, we need to find both the initial period tile index and the translation vector associated to a given tile $P_{i,j,k}$. Hence, thanks to Theorem 3, we have

$$\forall (i,j,k) \in \mathbb{Z}^3, P_{i,j,k} = T_W P_{i^0,j^0,k^0} \text{ with } W = w_0 U_0 + w_1 U_1 + w_2 U_2$$

and $0 \leq k^0 = \left\{ \frac{k}{\alpha_2} \right\} < \alpha_2$, $w_2 = \left\lfloor \frac{k}{\alpha_2} \right\rfloor$, $\quad 0 \leq j^0 = \left\{ \frac{j + w_2\beta_1^2}{\alpha_1} \right\} < \alpha_1$, $w_1 = \left\lfloor \frac{j + w_2\beta_1^2}{\alpha_1} \right\rfloor$,

$$0 \leq i^0 = \left\{ \frac{i + w_1\beta_0^1 + w_2\beta_0^2}{\alpha_0} \right\} < \alpha_0, \; w_0 = \left\lfloor \frac{i + w_1\beta_0^1 + w_2\beta_0^2}{\alpha_0} \right\rfloor.$$

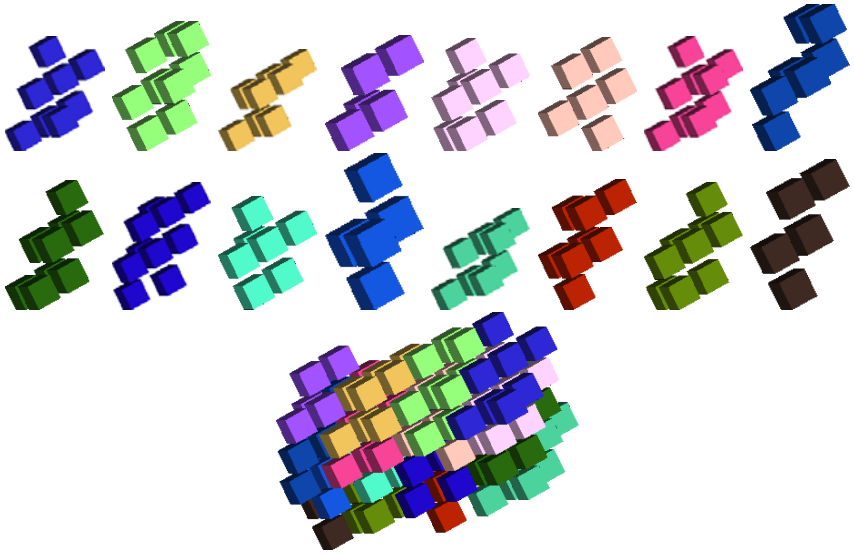

Fig. 4. All distinct tiles of a QAT in $\mathbb{Z}^3$ and its super-tile.

4 Experiments

The algorithms were implemented in both 2D and 3D, with different refinements in order to be able to compare the implementations. For details on the 2-D algorithms, refer to [7]. The `backward mapping` (`B. M.` for short) implementation let

Algorithm 4: QAT Algorithm in 3-D.

Input: A QAT (ω, M, V) and an image $g : [0, t_0] \times [0, t_1] \times [0, t_2] \to \mathbb{Z}$
Output: an image $h : [min_0, max_0] \times [min_1, max_1] \times [min_2, max_2] \to \mathbb{Z}$
Compute min_i and max_i quantities from t_i;
if *f dilating* **then**
  $f \leftarrow f^{-1}$;
  Compute the Hermite Normal Form of the matrix M;
  Compute the minimal periodicities $\{\alpha_0, \alpha_1, \alpha_2\}$ and vectors $\{\boldsymbol{U}_0, \boldsymbol{U}_1, \boldsymbol{U}_2\}$;
  Use Algorithm 3 to compute the canonical tiles in the super-tile $\mathcal{P}$;
  for $i \leftarrow 0$ **to** $t_0 - 1$ **do**
    for $j \leftarrow 0$ **to** $t_1 - 1$ **do**
      for $k \leftarrow 0$ **to** $t_2 - 1$ **do**
        Compute W, i^0, j^0, k^0 ;
        $h(T_W P_{i^0,j^0,k^0}) \leftarrow g(i, j, k)$;
else
  Compute the Hermite Normal Form of the matrix M;
  Compute the minimal periodicities $\{\alpha_0, \alpha_1, \alpha_2\}$ and vectors $\{\boldsymbol{U}_0, \boldsymbol{U}_1, \boldsymbol{U}_2\}$;
  Use Algorithm 3 to compute the canonical tiles in the super-tile $\mathcal{P}$;
  for $i \leftarrow min_0$ **to** $max_0 - 1$ **do**
    for $j \leftarrow min_1$ **to** $max_1 - 1$ **do**
      for $k \leftarrow min_2$ **to** $max_2 - 1$ **do**
        Compute W, i^0, j^0, k^0 ;
        $h(i, j, k) \leftarrow g(T_W P_{i^0,j^0,k^0})$;

	2-D - instructions (time in sec.)			
	`B.M.`	`simple`	`Periodicity`	`noMultiply`
contracting	1 607 774 (0.036)	64 536 315 (0.06)	29 578 702 (0.036)	27 679 044 (0.036)
isometry	63 058 160 (0.112)	57 619 374 (0.064)	39 682 795 (0.056)	35 875 892 (0.044)
dilating	391 622 017 (0.404)	185 956 768 (0.12)	87 490 567 (0.084)	83 472 387 (0.078)

	3-D - instructions (time in sec.)		
	`B.M.`	`simple`	`Periodicity`
contracting	15 864 982 (0.02)	47 303 861 (0.052)	12 865 125 (0.012)
isometry	750 102 224 (0.416)	51 121 827 (0.068)	15 234 007 (0.016)
dilating	170 072 035 547 (79.637)	2 479 676 409 (1.384)	7 760 893 011 (0.632)

	2-D (PSNR in dB)		3-D (PSNR in dB)	
	`B.M.`	`Periodicity`	`B.M.`	`Periodicity`
contracting	24.764	23.4823	17.8026	17.0304
isometry	27.7619	25.8052	19.4115	15.9481
dilating	31.2331	30.8375	20.4435	16.7862

Table 1. Comparative evaluation in 2-D and 3-D. The last table presents the PSNR evaluation of the composition $f \cdot f^{-1}$.

us compare the tile periodicity method with the widely used `backward mapping` method [9]. The `simple` implementation does not use tiles periodicity and uses algorithm 2 for each tile. The `periodicity` implementation uses the periodicity and the algorithm 4. The `noMultiply` implementation additionally uses a method presented in [4] which uses a handling of remains instead of computing a matrix product in 3. The experiments are performed on an Intel© Centrino© Duo T2080 (2 x 1.73 GHz) in monothread and we give on one hand the time of computation and on the other hand the number of elementary instructions. The QATs used are the following : In 2-D:

$$\left(\omega, \begin{pmatrix} 3 & -4 \\ 4 & 3 \end{pmatrix}, \begin{pmatrix} 0 \\ 0 \end{pmatrix}\right) \text{ where } \omega = \begin{cases} 10 \text{ for the contracting application} \\ 5 \text{ for the isometry} \\ 2 \text{ for the dilating application} \end{cases}$$

In 3-D:

$$\left(\omega, \begin{pmatrix} 9 & -20 & -12 \\ 12 & 15 & -16 \\ 20 & 0 & 15 \end{pmatrix}, \begin{pmatrix} 0 \\ 0 \\ 0 \end{pmatrix}\right) \text{ where } \omega = \begin{cases} 100 \text{ for the contracting application} \\ 25 \text{ for the isometry} \\ 4 \text{ for the dilating application} \end{cases}$$

The pictures are of size : 200 x 171 in 2-D and 10 x 10 x 10 in 3-D (simple cube).

Figure 5 illustrates the results in dimension 2. As expected, when comparing `B.M.` and `Periodicity`, results are similar for both contracting and isometry QATs. Differences appear when dilating QAT is considered. Indeed, since a unique color is associated to a tile in the `Periodicity` algorithm, the transformed image contains sharp edges (Fig 5-(l)) On the other hand, the interpolation process in the `B.M.` algorithm makes the image blurred. To compare the

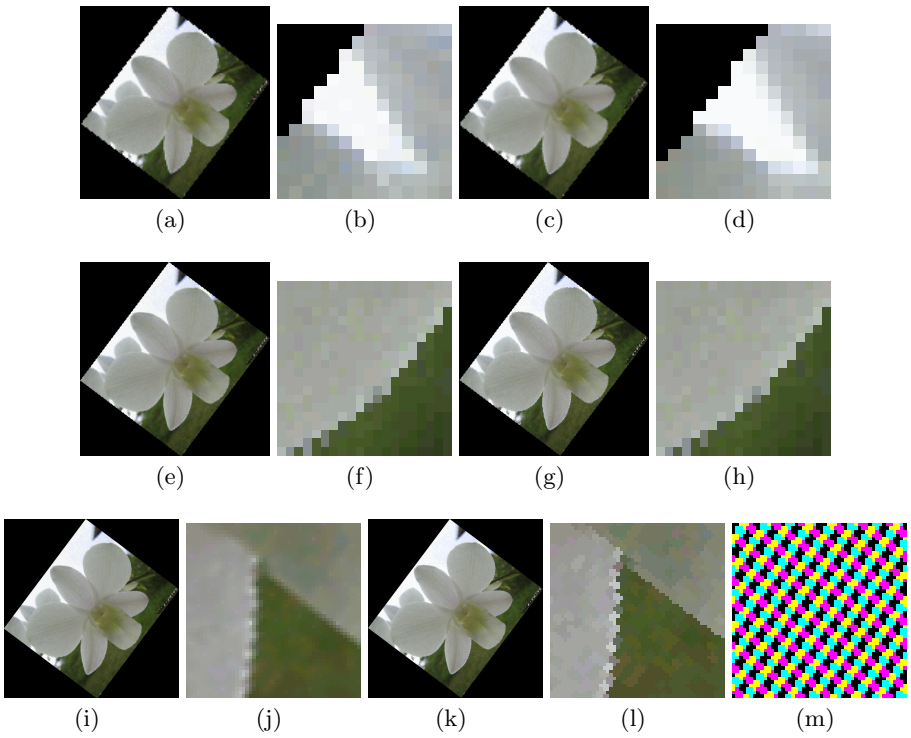

Fig. 5. Results in dimension 2: $(a-d)$ Contracting QAT (`B.M.` $(a-b)$ and `Periodicity` $(c-d)$); $(e-h)$ Isometry (`B.M.` and `Periodicity`); $(i-l)$ Dilating (`B.M.` and `Periodicity`). (m) illustrates the tile structure of the dilating QAT on the same square as in (l).

time efficiency (Table 1), we have considered two quantities: the total number of elementary operations of the main loop[5] and the overall computational time in seconds. Table 1 and Figure 6 present the results in dimension 3. For the sake of clarity, we have only considered an input binary image but the transformation algorithms can be applied to 3-D color images. We have also performed a peak signal-to-noise ratio (PSNR for short, given in decibel dB) computation between the input image in 2-D and 3-D, and the result of the composition $f.f^{-1}$. This test has been designed to evaluate the propagation of the error through the transformations with a signal processing tool. As presented in Table 1, the distortion induced by the proposed method is always smaller than the one induced by the backward mapping technique. Note that to have relevant measurements, we have used a density 3-D volume for the 3-D test (see Fig. 6-(h)).

[5] obtained with the `valgrind` profiling tool.

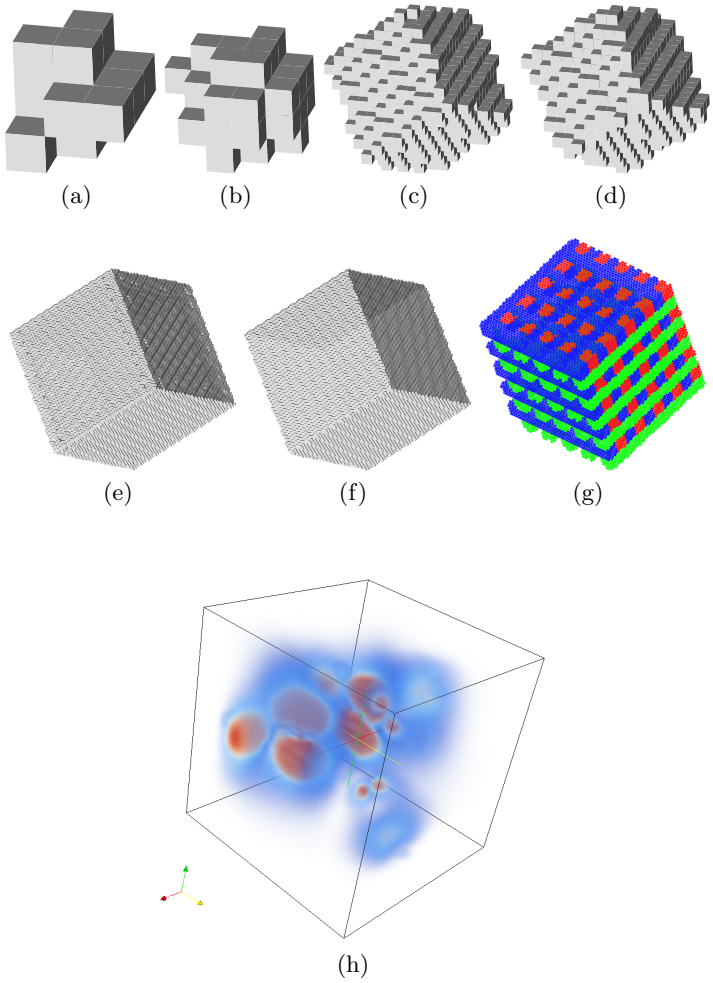

Fig. 6. Results in dimension 3: $(a-b)$ Contracting (`B.M.` and `Periodicity`), $(c-d)$ Isometry and $(e-f)$ Dilating (`B.M.` and `Periodicity`). (g) illustrates the tile structure of the dilating QAT. (h) is the $32 \times 32 \times 32$ density volume used in the $f.f^{-1}$ composition test (from the TC18 data-set `http://www.tc18.org`).

5 Conclusion and Future Works

In this paper, we have first re-demonstrated an existing result in dimension 2 with our formalism and provide a generalization in dimension 3 of fast image transformations with QAT. Compared to a classical image transformation technique, we have also illustrated the strength of such arithmetical methods to speed up transformations in higher dimensions. As detailed above and based on the generic $n-D$ transformation algorithm proposed in [6,7,8], we had to

perform specific computation to obtain the minimal periods in dimension 2 and 3. A very challenging future work is to define a framework to compute these minimal periods when a specific dimension is considered. In order to achieve this goal and instead of having explicit formulas, we plan to investigate an algorithmic solution based on the $n - D$ canonical tile counting algorithm proposed in [6]. Furthermore, in dimension 2 and 3, comparisons to other transformation algorithms, such as Fourier based technique, are also of interest.

References

1. Nehlig, P., Ghazanfarpour, D.: Affine Texture Mapping and Antialiasing Using Integer Arithmetic. Computer Graphics Forum **11**(3) (1992) 227–236
2. Jacob, M.: Transformation of digital images by discrete affine applications. Computers & Graphics **19**(3) (1995) 373–389
3. Nehlig, P.: Applications quasi affines: pavages par images réciproques. Theoretical Computer Science **156**(1-2) (1996) 1–38
4. Jacob, M.: Applications quasi-affines. PhD thesis, Université Louis Pasteur, Strasbourg, France (1993)
5. Jacob-Da Col, M.: Applications quasi-affines et pavages du plan discret. Theoretical Computer Science **259**(1-2) (2001) 245–269 english version: `http://dpt-info.u-strasbg.fr/~jacob/articles/paving.pdf`.
6. Jacob-Da Col, M.A., Tellier, P.: Quasi-linear transformations and discrete tilings. Theoretical Computer Science **410**(21-23) (2009) 2126 – 2134
7. Blot, V., Coeurjolly, D.: Quasi-affine transform in higher dimension. Technical Report RR–LIRIS-2009-010, Laboratoire LIRIS (April 2009) `http://liris.cnrs.fr/publis?id=3853`.
8. Blot, V., Coeurjolly, D.: Quasi-affine transform in higher dimension. In: 15th International Conference on Discrete Geometry for Computer Imagery. LNCS, Springer-Verlag (submitted).
9. Foley, J.D., van Dam, A., Feiner, S.K., Hughes, J.F.: Computer Graphics: Principles and Practice. second edn. Addison-Wesley, Reading, Mass. (1990)
10. Storjohann, A., Labahn, G.: Asymptotically fast computation of hermite normal forms of integer matrices. In: ISSAC '96: Proceedings of the 1996 international symposium on Symbolic and algebraic computation, New York, NY, USA, ACM (1996) 259–266